INTERNATIONAL JOURNAL FOR NUMERICAL METHODS IN FLUIDS
Int. J. Numer. Meth. Fluids **28**: 841–857 (1998)

IMPROVED LAMINAR PREDICTIONS USING A STABILISED TIME-DEPENDENT SIMPLE SCHEME

I.E. BARTON*

Division A, Department of Engineering, University of Cambridge, Trumpington Street, Cambridge CB2 IPZ, UK

SUMMARY

A new scheme which can solve unsteady incompressible flows is described in this paper. The scheme is a variant of the SIMPLE methodology. Typically, a scheme of this type tends to suffer from stability problems, which this new scheme overcomes by taking small intermediate steps within a time step. The calculations made in the intermediate steps are damped to enhance the stability of the scheme. The new stabilised scheme is evaluated for laminar flow around a square cylinder, impulsively started laminar flow over a backward-facing step and fluctuating laminar flow over a backward-facing step. Comparisons are made with other numerical predictions and experimental data. In general, good agreement is found, except for the fluctuating laminar flow over a backward-facing step problem. The new scheme is found to have the same level of accuracy, stability and efficiency in comparison with the PISO scheme, but it is easier to code. © 1998 John Wiley & Sons, Ltd.

KEY WORDS: SIMPLE scheme; PISO scheme; transient flow

1. INTRODUCTION

The numerical solution of incompressible fluid flow problems can be achieved in a number of ways in primitive variables, and consequently, there have been a variety of solution schemes proposed [1–10]. The fundamental difficulty is in how the velocity and pressure fields are coupled together. The majority of the solution methodologies devised tend to be for solving steady state problems. This probably reflects the fact that the majority of applications undertaken are steady state problems. The three most commonly used schemes are based on variants of the marker and cell (MAC) [11] devised by Harlow and Welch [1], the semi-implicit method for pressure linked equations scheme (SIMPLE) developed by Patankar and Spalding [2] and the pressure implicit with splitting operators (PISO) scheme devised by Issa [5]. An alternative approach to using primitive variables is to rearrange the governing equations so that pressure is no longer a dependent variable, e.g. vorticity–streamfunction notation [12,13], but this approach is not readily applicable to complex flow problems or three-dimensional problems.

The current research concerns the SIMPLE and PISO schemes, where an unsteady state variant of SIMPLE is developed. The SIMPLE scheme was initially established by various authors [2,3,14,15], and is presented in great detail in Patankar [16]. The scheme was originally

* Correspondence to: Division A, Department of Engineering, University of Cambridge, Trumpington Street, Cambridge CB2 1PZ, UK.

CCC 0271–2091/98/150841–17$17.50

Received March 1997
Revised September 1997

formulated to solve steady state problems. The development of the scheme for unsteady state problems has been developed [17–20]. The original formulation uses a pseudo time-derivative in order to underrelax the scheme. This approach essentially amounts to local time stepping [3,21]. In comparison, the PISO scheme [5,22] was developed to solve transient problems using real time stepping. Generally speaking, the SIMPLE and PISO schemes have strong similarities, both in terms of algorithmic formulation and general methodology.

The SIMPLE scheme has been enhanced in a number of ways by others, some recent enhancements include a non-staggered formulation using a finite difference approach [23]. Multigrid techniques have been incorporated [24], as well as a multigrid solvers [25]. The original formulations of the SIMPLE scheme used Cartesian grid systems, however, body fitted co-ordinates are now very popular [26,27] and the finite element method has been used with the SIMPLE scheme [28]. Enhancements made to the SIMPLE-type methodologies have been reviewed elsewhere [29–31].

The original PISO scheme devised by Issa [5] has also been developed, though mainly for combusting flows [22,32,33]. This includes combusting particulate flows [34]. The application of the multigrid method has been applied to PISO, again for a combustion chamber application [9]. Dukowicz [35] presented an example of particulate time-dependent flow with a Monte Carlo simulation for particle dispersion. The most suitable application of the source term for turbulent flows using the SIMPLE and PISO schemes is investigated in Wanik and Schnell [17].

The present investigation is a continuation from Barton [20], where the SIMPLE and PISO variants were tested for an unsteady state flow problem. A SIMPLE variant scheme called scheme (2) in Barton [20], which is referred to as SIMPLE2 in the present paper, was found to predict solutions as accurately as the PISO scheme, in addition to having a similar computational cost when using the same time step, but the scheme was found to be less stable than the PISO scheme. In the present research, the SIMPLE2 scheme is developed so that it is made as stable as the PISO scheme. The need to develop such a scheme is that the SIMPLE methodology does not have velocity correction terms, which can be complex to derive for non-Cartesian grid systems. Also, in principle, it has the benefit that additional partial differential governing equations can be coupled with the solution of the velocity and pressure fields to a greater degree. The present research does not examine this premise. The new scheme is referred to as SIMPLE*.

2. NUMERICAL ANALYSIS

The governing equations for planar, unsteady, constant density flow can be described by simplified Navier–Stokes equations and the equation of continuity. These equations are expressed as

$$\frac{\partial \rho u}{\partial t}+\frac{\partial \rho u^2}{\partial x}+\frac{\partial \rho uv}{\partial y}=-\frac{\partial p}{\partial x}+\frac{\partial}{\partial x}\mu\frac{\partial u}{\partial x}+\frac{\partial}{\partial y}\mu\frac{\partial u}{\partial y}, \tag{1}$$

$$\frac{\partial \rho v}{\partial t}+\frac{\partial \rho uv}{\partial x}+\frac{\partial \rho v^2}{\partial y}=-\frac{\partial p}{\partial y}+\frac{\partial}{\partial x}\mu\frac{\partial v}{\partial x}+\frac{\partial}{\partial y}\mu\frac{\partial v}{\partial y}, \tag{2}$$

$$\frac{\partial \rho u}{\partial x}+\frac{\partial \rho v}{\partial y}=0, \tag{3}$$

where ρ is the density and μ is the viscosity of the flow. The governing equations are solved in primitive form (u, v, p). The first step in the solution procedure is to discretise the above

governing equations, applying conventional differencing to the partial derivative terms, e.g. refer to Reference [36]. In general form, this can be expressed as

$$\left(A_{P,u}^{n*} + \alpha\frac{\rho}{\Delta t}\right)u_P^{n+1} = \sum_M A_{M,u}^{n*}u_M^{n+1} - \Delta_x p^{n+1} + (\beta u_P^n + \gamma u_P^{n-1})\frac{\rho}{\Delta t}, \tag{4}$$

$$\left(A_{P,v}^{n*} + \alpha\frac{\rho}{\Delta t}\right)v_P^{n+1} = \sum_M A_{M,v}^{n*}v_M^{n+1} - \Delta_y p^{n+1} + (\beta v_P^n + \gamma v_P^{n-1})\frac{\rho}{\Delta t}, \tag{5}$$

$$\Delta_x(\rho u)^{n+1} + \Delta_y(\rho v)^{n+1} = 0. \tag{6}$$

The A coefficients contain the discretised flux terms and diffusion terms. These terms have been derived elsewhere [16,37] and do not require any further elucidation here. The M index represents the nodes surrounding the pole node incorporated from the discretisation procedure. The A coefficients in the above notation have a superscript $n*$, which represents the time-level of the velocity terms used in their construction. This new notation is introduced because previous formulations of the SIMPLE and PISO scheme apply 'linear implicit treatment' to terms such as u^2. This term therefore, becomes $u^n u^{n+1}$. The u^n term is then used in the construction of the A coefficients and the u^{n+1} term is used in the solution algorithm. As the SIMPLE2 and the SIMPLE* scheme presented later, updates the coefficient terms, the present research specifically states what velocity terms form the construction of the A coefficients.

The time derivative is constructed from the α, β, γ terms. Crank–Nicolson differencing [38] is achieved by the respective substitution of $(1, 1, 0)$ and one-sided forward differencing [39] (OSFD) is achieved by the respective substitution of $(3/2, 2, -1/2)$. Both schemes are second-order-accurate, based around different time levels; where Crank–Nicolson is based on the $n+1/2$ time level and OSFD is based on the $n+1$ time level.

The momentum equations (4) and (5) are further simplified in order to present the PISO, SIMPLE2 and SIMPLE* schemes. These two equations are represented by a single equation, where U can be replaced by either u or v. Also, the time-derivative terms have been incorporated into the A_P coefficient and the source term S_u.

$$A_P^{n*}U_P^{n+1} = \sum A_M^{n*}U_M^{n+1} - \Delta p^{n+1} + S_u. \tag{7}$$

The numerical calculations used a second-order upwind differencing (SOUD) scheme [40]; however, the algorithms presented could be applied to a number of differencing and interpolation schemes. For example, the hybrid differencing scheme [41], has been extensively applied to the SIMPLE and PISO schemes.

The outlet condition was found by extrapolation. First-order and quadratic extrapolations recommended by Peric [42] were found to give fairly poor solutions in the outlet region. The outflow boundary condition developed and discussed in Barton [21] was applied. In short, the extrapolated velocities at the outlet are calculated using the following fit,

$$u = A + \frac{B}{(x/\Delta x)} + \frac{C}{(x/\Delta x)^2}. \tag{8}$$

In the extrapolation, the four velocity positions upstream of the outflow boundary are used. The velocity position the furthest from the outflow boundary is used as the datum position for x. The velocity values at the other three positions are used for extrapolation calculation. The Δx term is the cell length adjacent to the outflow boundary. Therefore, if uniform cells are used near the exit region, the extrapolated velocity value is estimated by (using compass notation),

$$u_{\text{exit}} = \frac{27u_w - 12u_{ww} + u_{www}}{16}, \tag{9}$$

and is then corrected to ensure that overall flux is conserved. This formulation appears to reduce numerical errors near the outflow boundary.

Similar to other numerical studies, prescribed velocity profiles are set at the inlet. No-slip boundary conditions are applied at the wall boundaries.

The discretised equations form a matrix that is solved using the tri-diagonal matrix algorithm [38] (TDMA). The algorithm sweeps through the solution domain a fixed number of times. If, however, the matrix array is solved to an accuracy of at least 0.1% of the maximum change, then the matrix solution procedure is terminated for that iteration.

3. THE NUMERICAL SOLUTION PROCEDURES

The PISO, SIMPLE2 and SIMPLE* schemes are outlined below.

3.1. The PISO scheme

The standard PISO scheme is detailed in Issa [5]. Issa also discusses the similarities and differences of the PISO algorithm compared with the SIMPLE algorithm. Both schemes solve the pressure field by ensuring mass continuity is satisfied. Also, both schemes use the basic algorithmic formulation of initially predicting the velocity field based on the current pressure field, and then correcting the pressure and velocity fields so they satisfy mass continuity. This is achieved in the following steps:

Step l. Predict velocities based on the momentum equations and the previously calculated pressure field.

$$A_P^n U_P^* = \sum A_M^n U_M^* - \Delta p^n + S_u. \tag{10}$$

Step 2. Predict pressure and velocities in order to satisfy continuity. This is achieved using the following equation:

$$A_P^n U_P^{**} = \sum A_M^n U_M^* - \Delta p^* + S_u. \tag{11}$$

From the previous step one obtains

$$U_P^{**} = U_P^* - \Delta(p^* - p^n)/A_P^n. \tag{12}$$

Next, assuming that Equation (12) must obey continuity, this is substituted into Equation (6), which leads to the following equation

$$\Delta_x(\rho u)^* + \Delta_y(\rho v)^* = \Delta_x(\Delta_x(p^* - p^n)/A_{P,u}^n) + \Delta_y(\Delta_y(p^* - p^n)/A_{P,v}^n), \tag{13}$$

which is the first Poisson equation used to predict the pressure field. After its solution, values of p^* can be substituted into Equation (12) and the terms u_p^{**} and v_p^{**} can be calculated. The next step is similar to the previous step.

Step 3. Correct the pressure and velocities such that continuity is satisfied, using the following equation

$$A_P^n U_P^{***} = \sum A_M^n U_M^{**} - \Delta p^{**} + S_u. \tag{14}$$

Again, taking this equation away from the previous step, the following equation is obtained, similar to Equation (12),

$$U_P^{***} = U_P^{**} + \sum A_M^n (U_M^{**} - U_M^*)/A_P^n - \Delta(p^{**} - p^*)/A_P^n. \tag{15}$$

In this case, however, there are velocity correction terms, which further complicates the next Poisson pressure equation that is derived and solved.

The original PISO scheme, as presented by Issa [5], uses the Crank–Nicolson scheme for the time-derivative. Kim and Benson [43], however, apply OSFD to the PISO scheme arguing that this will improve the solution from first-order-accurate to second-order-accurate for the temporal terms. In Barton [20], the PISO scheme was found to exhibit greater accuracy with the Crank–Nicolson scheme compared with the OSFD scheme, which contradicts Kim and Benson's argument. Although, the pressure gradient is implicitly treated, this is not true for all of the velocity terms, i.e. u^2 terms become $u^n u^{n+1}$. It is therefore, straightforward to show that a second-order approximation of $u^n u^{n+1}$ is given by $(u^{+1/2})^2$. If these terms dominant the flow, then the Crank–Nicolson scheme is second-order-accurate. The current research uses the Crank–Nicolson scheme for the PISO algorithm.

3.2. The SIMPLE2 scheme

This scheme is detailed in Barton [20], as scheme (2). It follows the standard SIMPLE methodology using real time-derivatives. The scheme exactly follows the same first two steps of the PISO scheme described above. The next two steps are a repetition of the Steps 1 and 2, except using updated coefficients and pressure field. Steps 3 and 4 are given as:

Step 3. Correct the velocities based on the momentum equations using the updated pressure field;

$$A_P^{**} U_P^* = \sum A_M^{**} U_M^* - \Delta p^* + S_u. \tag{16}$$

Step 4. Correct the pressure and velocities in order to satisfy continuity using the discretised equation of continuity and the following equation,

$$A_P^{**} U_P^{**} = \sum A_M^{**} U_M^* - \Delta p^{**} + S_u. \tag{17}$$

The advantage of the SIMPLE2 scheme is that it does not require the solution of velocity correction terms. The pressure field is predicted and corrected similar to the PISO scheme. The SIMPLE2 scheme requires four steps in its solution. In contrast, PISO only requires three steps; however, the required CPU is not that much greater than the PISO scheme because approximately 80% of the required CPU time is spent solving the pressure field. In Barton [20], the SIMPLE2 scheme was found to predict more accurate results using the OSFD scheme instead of the Crank–Nicolson scheme. This possibly suggests that the u^2 terms are being solved closer to the form of $(u^{n+1})^2$ rather than $(u^{n+1/2})^2$. For the two test cases predicted in Barton [20], the maximum time step the SIMPLE2 scheme could use without predicting divergent results was approximately half the value of the PISO scheme for flow around a square cylinder, and a tenth of the value for flow over a backward-facing step. Clearly, the stability of the scheme requires improvement. This is achieved in SIMPLE*.

3.3. The SIMPLE* scheme

The SIMPLE* scheme is a continuation of the SIMPLE2 scheme, where the SIMPLE routine is repeated a number of times; however, between each cycle certain terms are underrelaxed. In order for the scheme to remain time-accurate, the last solution must be free from underrelaxation. For the scheme, N needs to be defined as the total number of internal cycles and I as the current internal cycle number. This means for the first internal cycle $I = 1$; therefore, a coefficient with a superscript of 0 refers to a previous external time step value. Now, the scheme can be described as

Cycle (I), Step 1. Predict velocities based on the momentum equations.

$$A_P^{(I-1)} ** U_P^{I} * = \sum A_M^{(I-1)} ** U_M^{I} * - \Delta p^{(I-1)} + S_u. \tag{18}$$

After the above set of equations is solved, underrelax the solution in the following manner:

$$U_P^{I} *^{\mathrm{NEW}} = U_P^{I} *^{\mathrm{OLD}} \alpha_U + U_P^{(I-1)} *(1 - \alpha_U), \tag{19}$$

where $\alpha_U = \min[I/(N-1), 1]$. Note, U_p^0* is taken to be the previous velocity solution. Also, the underrelaxation parameters from Equation (19) are not introduced into Equation (18), as Raithby and Schneider [3] do in their formulation of SIMPLE, but directly afterwards. This is important when the pressure correction equation is formed by taking Equation (20) away from Equation (18). The underrelaxation parameter is dependent on the internal cycle number; this initially dampens out spurious results, but the final two cycles have a value of unity, allowing the solution to remain time-accurate.

Cycle (I), Step 2. Predict the pressure correction field and correct the velocity fields with the following equation taken away from Equation (18); which is substituted into the discretised equation of continuity, therefore, the same derivation previously discussed for the PISO and SIMPLE2 schemes is again applied,

$$A_P^{(I-1)} ** U_P^{I} * = \sum A_M^{(I-1)} ** U_M^{I} * - \Delta p^{I} + S_u. \tag{20}$$

The pressure correction terms are therefore in the form:

$$pc^I = p^I - p^{I-1}. \tag{21}$$

These pressure correction terms are not underrelaxed when applied to the velocity correction relationship, but they are when applied to the pressure field, e.g.

$$p^I = p^{I-1} + pc^I \alpha_p. \tag{22}$$

In this case, the underrelaxation parameter is given by $\alpha_p = \min[(I/(N-1))^2, 1]$. Note that the previous underrelaxation for the velocity terms is linear, whereas, the updated pressure field is non-linearly underrelaxed. Divergent results were found to be dominated by the pressure field calculation and to a lesser degree in the velocity calculation; whereas the velocity corrections played an insignificant role. Therefore, the pressure field is strongly relaxed for the initial cycles, with no underrelaxation applied on the final two cycles, again to ensure time-accuracy. Note that the SIMPLE* scheme is a generalisation of the SIMPLE2 scheme; if $N = 2$, then the two schemes are the same.

Taking an overview of the SIMPLE* scheme, it would appear that the scheme requires approximately $N/2$ times greater CPU time for a solution compared with the PISO scheme. This is true if the pressure correction field is solved to the same degree of accuracy per cycle;

however, the internal cycles do not require an accurate solution where small approximate steps to the final solution of the cycle are acceptable. Therefore, the matrix solution algorithm does not have to be applied to the same degree of accuracy. For example, using the sweeping TDMA solution procedure [38], 100 sweeps may be required for a successful application of the PISO scheme, whereas using the SIMPLE* scheme, approximately $100/N$ sweeps may only be required to achieve the same degree of accuracy, if not better. This is because the pressure field is solved with the same number of sweeps converging to a solution on each internal cycle.

4. EXAMPLE APPLICATIONS

The schemes presented are applied to two example applications, laminar flow over a backward-facing step and laminar flow around a square cylinder, as a validation exercise. These two applications were selected because the first one is an example of a steady state problem, while the second is an unsteady state problem, where vortices are shed downstream of the cylinder. Finally, a simulation using a fluctuating inlet velocity profile over a backward-facing step is presented as a demonstration exercise.

4.1. Flow over a backward-facing step

A backward-facing step is one of the most simple geometries where flow separation and reattachment occur. The present research considers a flow which has an upper fixed wall boundary, a similar configuration is experimentally and numerically studied by Armaly *et al.* [44]. The upper boundary simplifies the boundary conditions and consequently, the problem has a popular numerical problem. Computations of a backward-facing step geometry have been carried out by a large number of authors [8,12,13,44–51]. All these studies have investigated an enclosed backward-facing step where the geometry is similar to the present study. The flow configuration is illustrated in Figure 1. The expansion number is 2, where the expansion number is defined as the ratio of the main channel height to the inlet channel height. The problem applies a parabolic u-velocity profile at the inlet. The Reynolds number is defined using twice the inlet channel height, $2h$, the average inlet velocity and the fluid's dynamic viscosity. This definition is the same as in the study by Armaly *et al.* [44]. The problem domain used in the calculations is 40 step heights long in the main channel, two small inlet of channels of $0.1h$ and $1.2h$ are tested. The outlet condition discussed in Section 2 is applied to the outlet boundary, and no-slip boundary conditions are applied at the walls.

The computations are undertaken on a non-uniform Cartesian grid system. The grid system uses 70×50 grid points and 80×50 for the longer inlet channel geometry. There is grid refinement close to the walls, including the step wall. A similar grid distribution was tested for

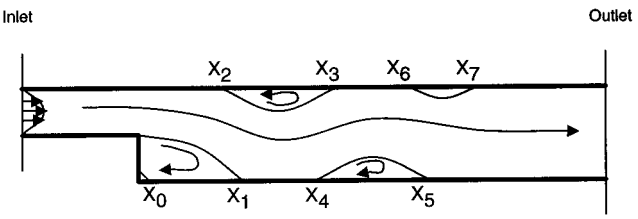

Figure 1. Illustration of the flow over a backward-facing step, showing several recirculation regions attached to the upper and lower walls. The labelling system of the reattachment and separation positions is depicted.

Table I. Steady state numerical predictions of the main reattachment and separation positions at an inlet Reynolds number of $Re = 800$

	x_1	x_2	x_3
Present results	12.19	9.75	20.89
Barton [51]	12.03	9.64	20.96
Sani and Gresho [50]	12.44	10.18	20.50
Gartling [48]	12.20	9.70	20.95

grid independency in Barton [54]. Therefore, the differences should be typically $< 1\%$ for the finest grid results. The largest differences tend to occur for the separation length, x_2, for some of the higher Reynolds numbers; the differences between the two sets of results are of the order of 2%. Spatial errors are not an essential consideration in the present study, as interest is in the time-dependent behaviour of the schemes that can be observed, provided spatial errors are not a dominant factor. Although, for this particular problem compared with the laminar flow around a square cylinder, obtaining accurate predictions is of greater interest as there is a consensus of opinion of what are the correct flow characteristics.

4.1.1. A steady state problem. Initially, the classical backward-facing step problem recommended by Gresho [52] is investigated. The problem sets the inlet Reynolds number to $Re = 800$. Gresho *et al*. [53] have established that the flow is steady for inlet Reynolds numbers up to $Re = 800$, using a variety of numerical schemes, but have not established when the flow becomes unstable. Furthermore, the experimental results [44] become transitional at $Re = 1200$. This indicates that the problem should converge to a steady state solution. There are numerous steady state predictions for this problem, and a recent review is given in Barton [54]. It is sufficient to say that recent accurate predictions have been detailed in Gartling [48], Sani and Gresho [50] and Barton [51]. The current predictions of the reattachment and separation positions, x_1, x_2 and x_3 at $T = 200$, where T is non-dimensionalised time, are compared with the steady state predictions of Gartling [48], Sani and Gresho [50] and Barton [51] in Table I. The growth of the recirculation regions appears be to finished for times greater than $T = 200$, and well established by $T = 100$. The numerical results shown in the table are taken from the results that use the finest grid and best outlet treatment in their particular study. There are only minor discrepancies in the present results compared with other predictions.

4.1.2. Growth of recirculation regions problem. The growth of the main recirculation regions is investigated for an impulsively started flow. The start-up flow conditions set the pressure field to zero, and a parabolic u-velocity profile at the inlet. The rest of the u-velocity field is set to the value of half the maximum inlet velocity, and the start-up conditions for the v-velocity field is set to zero. The simulation therefore, has to cope with introducing the pressure field and introducing viscous effects into the velocity field. The start-up flow conditions allow for initial rapid growth of the reattachment and separation positions.

The problem was tested to find the maximum time step applicable without producing divergent results. It was found that both the SIMPLE* and PISO schemes could successfully predict results using a non-dimensionalised time step of $\Delta T = 0.2$. The maximum time step the SIMPLE2 scheme could be applied to was $\Delta T = 0.03$. A set of results using the SIMPLE* scheme and a time step of $\Delta T = 0.002$, was run for 50 time units. These results are compared with predictions form the PISO, SIMPLE2 and SIMPLE* schemes using a time step value of

Table II. Prediction of the growth of the main reattachment and separation positions with time, using the small lip geometry

	SIMPLE* ($\Delta T = 0.002$)			PISO ($\Delta T = 0.03$)			SIMPLE2 ($\Delta T = 0.03$)			SIMPLE* ($\Delta T = 0.03$)		
T	x_1	x_2	x_3	x_1	x_2	x_3	x_1	x_2	x_3	x_1	x_2	x_3
10	5.62	3.98	9.57	5.74	7.58	9.54	5.61	3.96	9.58	5.62	3.98	9.57
20	7 l2	5.26	12.73	6.93	8.06	10.11	7.12	5.25	12.73	7.13	5.26	12.73
30	8.15	6.10	15.10	7.10	8.17	9.98	8.15	6.10	15.10	8.16	6.11	15.10
40	8.93	6.82	16.88	7.29	8.43	10.16	8.92	6.81	16.88	8.93	6.82	16.88
50	9.55	7.37	18.24	7.586	8.72	10.43	9.55	7.37	18.24	9.55	7.38	18.24

$\Delta T = 0.03$. The positions of the reattachment and separation positions x_1, x_2 and x_3 are shown in Table II at various times. The results show that the present predictions have not reached their steady state solution, which, as previously discussed, requires about 200 time units.

The results in Table II are a matter of concern as the SIMPLE2 and the SIMPLE* schemes predict dramatically different results compared with PISO. Note that this is not dependent on the time step. First, as can be seen from Table II, the SIMPLE* scheme using a small time step agrees well with the SIMPLE2 and SIMPLE* results using a larger time step. Second, the PISO scheme was also tested using a small time step and was found to produce similar results compared with the results using a larger time step. (At least this aspect of the both schemes is satisfactory). The differences in the PISO scheme compared with the SIMPLE2 and SIMPLE* schemes results were found to be caused by the inlet boundary reflecting pressure waves from the growth of the upper recirculation region. This can be prevented by making the dimensions of channel longer. The results in Table III show that the results from the PISO scheme and the SIMPLE* scheme using a long inlet channel are virtually identical. In addition, good agreement between these sets of results and the results using a small lip with the SIMPLE* scheme is obtained.

As the current research is interested in the time-dependent behaviour of the various schemes, the current results are not tested for grid independency. This is because the implicit nature of the various schemes can be observed, despite any spatial errors being present. Nevertheless, from a previous study using a similar grid resolution and the same differencing scheme [54], it can be inferred that the current set of results are grid-independent.

The fine time step results using the SIMPLE* scheme are compared with the predictions of Durst and Periera [55]. This is not strictly legitimate, because the two sets of predictions use different start-up conditions and slightly different geometries, flow configurations and inlet

Table III. Prediction of the growth of the main reattachment and separation positions with time, using a long inlet channel

	PISO			SIMPLE*		
T	x_1	x_2	x_3	x_1	x_2	x_3
10	5.58	3.88	9.42	5.55	3.86	9.41
20	7.05	5.18	12.62	7.03	5.17	12.61
30	8.04	6.01	15.01	8.03	6.00	15.00
40	8.79	6.68	16.79	8.78	6.68	16.78
50	9.39	7.18	18.14	9.38	7.18	18.14

Table IV. Prediction of the growth of the main reattachment and separation positions with time for the problem studied by Durst and Pereira [55] where the inlet velocity is slowly increased

T	x_1	x_2	x_3
10	4.2	3.1	5.8
20	5.6	4.7	8.9
30	6.5	4.8	10.7
40	7.6	5.2	13.1

conditions. Durst and Pereira use a longer inlet channel and smaller expansion number, but probably more importantly a different start-up solution. Even so, the growth of the various reattachment and separation positions appear to follow the same behaviour; where the main reattachment position, x_1, initially grows rapidly with time until a second eddy forms downstream. After a period of $T = 40$ from the start, the second eddy dies. The upper recirculation region grows in size and moves downstream with time. Initially, there is the creation of two minor recirculation regions: one forming a small recirculation region inside the main upper recirculation region and the other far downstream as the pressure finally recovers. Table IV shows the growth of the main reattachment and separation positions with time for the predictions by Durst and Pereira [55].

4.2. *Unsteady laminar flow around a square cylinder*

The problem of flow around a square cylinder, at a free stream Reynolds number of $Re = 250$ is predicted. This problem has been previously studied [20,56–58]. The cylinder diameter is D. The present problem domain sets the inlet boundary $3D$ upstream of the cylinder and the outlet boundary $10D$ downstream of the cylinder. The upper and lower boundaries are set at $8D$ away from the cylinder. A uniform velocity profile is set at the inlet boundary. The upper/lower boundary set $\mathrm{d}u/\mathrm{d}y = 0$ and $v = 0$ across it. The outlet condition outlined in Section 2 is used. The flow configuration is illustrated in Figure 2. The grid system is 50×50 in size, with very close refinement at the walls. Temporal datum results are predicted using a time step of $\Delta T = 0.005$ and the PISO and SIMPLE2 schemes (these results are identical to at least three orders of magnitude). The results in Table V show the flow

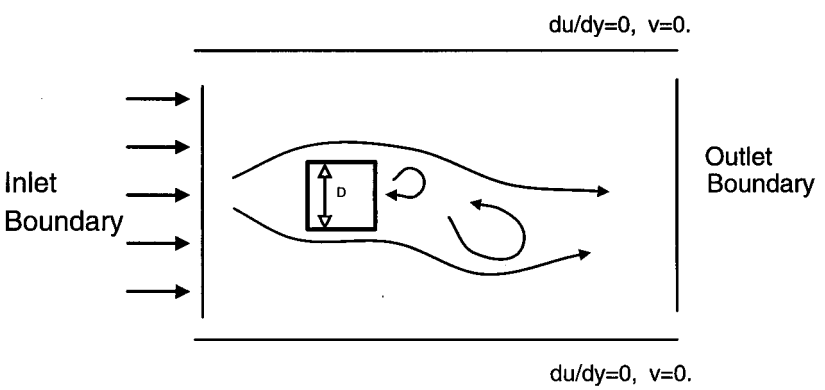

Figure 2. Illustration of flow around a square cylinder, showing an impression of vortex shedding behind the cylinder.

Table V. The predicted flow characteristics for the flow around a square cylinder problem[a]

	C_L^{MAX}	C_L^{MIN}	T_L	C_D^{MAX}	C_D^{MIN}	C_D^{AVE}	T_D
Datum	1.008	−1.001	6.014	1.876	1.618	1.744	6.010
PISO	0.986	−0.891	6.183	1.834	1.621	1.727	6.188
SIMPLE2	0.906	−0.901	6.062	1.840	1.612	1.725	6.067
SIMPLE*	0.915	−0.910	6.067	1.847	1.611	1.729	6.078

[a] Includes the lift coefficient C_L and its period T_L, as well as the drag coefficient C_D and its period T_D.

characteristics using the PISO, SIMPLE2 and SIMPLE* schemes using a time step of $\Delta T = 0.05$. This time step value is sufficiently small to capture the physics of the flow, but also sufficiently large to demonstrate temporal numerical diffusion. The SIMPLE* scheme is tested with the OSFD scheme. The flow characteristics include the maximum and minimum lift coefficients, C_L^{MAX} and C_L^{MIN}; the maximum, minimum and average drag coefficients, C_D^{MAX}, C_D^{MIN} and C_D^{AVE} well as the period of the lift oscillation, T_L, and the period of the complete drag oscillation, T_D. The Strouhal number is the inverse of T_L.

The streamlines of the SIMPLE* results are shown in Figure 3 for the non-dimensionalised time intervals of 5, 10, 15, 20, 35, 50, 65, 80, 95. The results show that the impulsively started flow almost immediately separates, forming two recirculation regions, which are also identical in size. The recirculation regions start to grow in size with time until the system finally becomes unstable and a vortex is shed. The flow then sheds vortices in an oscillatory manner from the top and bottom separation points behind the cylinder. The vortices one shed from the cylinder rapidly dissipate forming a considerable effect in the wake, which causes an oscillatory drag effect on the upper and lower surfaces of the cylinder.

The lift coefficient and period of the lift cycle, as well as drag coefficient and period of the drag cycle, are presented in Table V, similar analysis is undertaken [20]. In addition, Table VI presents the computational efficiency in the form of the CPU run time per iteration, R_c, as well as the maximum time step value that can be applied without predicting divergent results. The results show that a slightly better accuracy is achieved using the SIMPLE2 scheme followed by the SIMPLE* and PISO schemes. The quickest scheme is the PISO; however, the CPU run times are similar. The stability of the SIMPLE2 scheme is close to the SIMPLE* and PISO schemes for this particular problem. Stability is problem-dependent and it is likely that the maximum time step applicable is more a reflection of the physics of the flow than the numerical stability of the schemes.

4.3. Fluctuating laminar flow over a backward-facing step

As a demonstration exercise, fluctuating laminar flow over a backward-facing step is predicted. This problem has been experimentally studied by Sobey [59]. In the current problem, flow accelerates and then decelerates to a halt for a single cycle. The current interest in this problem is to establish the correct conditions required to generate a vortex sheet in the channel. The geometry with the long inlet channel used in Section 4.1 is also used in the current problem. The only difference is the inlet profile fluctuates in magnitude, so that the inlet u-parabola profile varies with time, such that

$$u(t) = u_{INLET} \sin 2\pi\omega t. \tag{23}$$

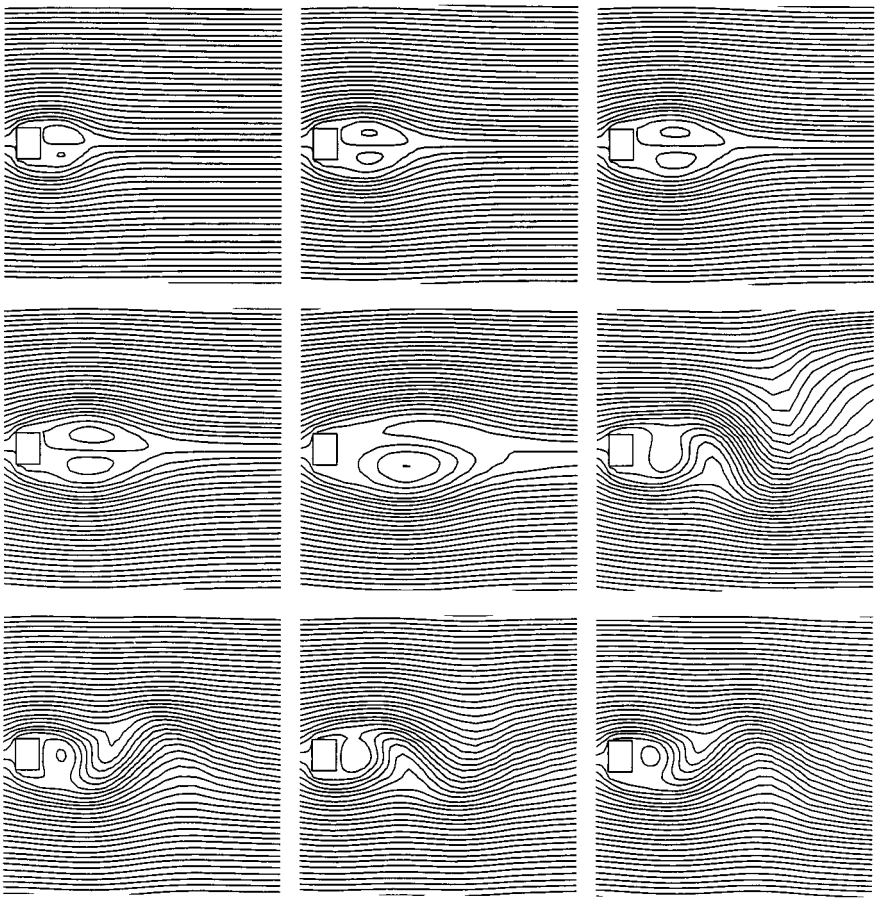

Figure 3. Predictions of the streamlines for flow around a square cylinder taken from an impulsive start using the SIMPLE* scheme, the illustration respectively shows streamline results for the non-dimensionalised times of 5, 10, 15, 20, 35, 50, 65, 80 and 95.

The frequency of oscillation is set to $\omega = 1.0$ Hz, and the simulation is run for 0.5 s using the SIMPLE* scheme, where $N = 10$ and $\Delta t = 5 \times 10^{-5}$ s, the non-dimensionalised time step is $\Delta T = 0.004$. The Reynolds number is set to $Re = 320$, based on the mean inlet velocity, and the Strouhal number is set to $St = 0.012$. The definition of these flow parameters are four times higher than Sobey [59], where the half step height is used as a length scale. The same geometry and flow configuration used in Sobey is modeled, where the step height is set to 1 mm and

Table VI. Results for the flow around a square cylinder problem, showing the accuracy of the lift and drag coefficients, the required CPU time per iteration and maximum time step

	σ_L	σ_D	R_c (s)	ΔT_{MAX}
PISO	5.14×10^{-2}	8.46×10^{-3}	1.89	0.1
SIMPLE2	3.08×10^{-2}	6.76×10^{-3}	2.07	0.06
SIMPLE*	4.18×10^{-2}	7.00×10^{-3}	2.22	0.1

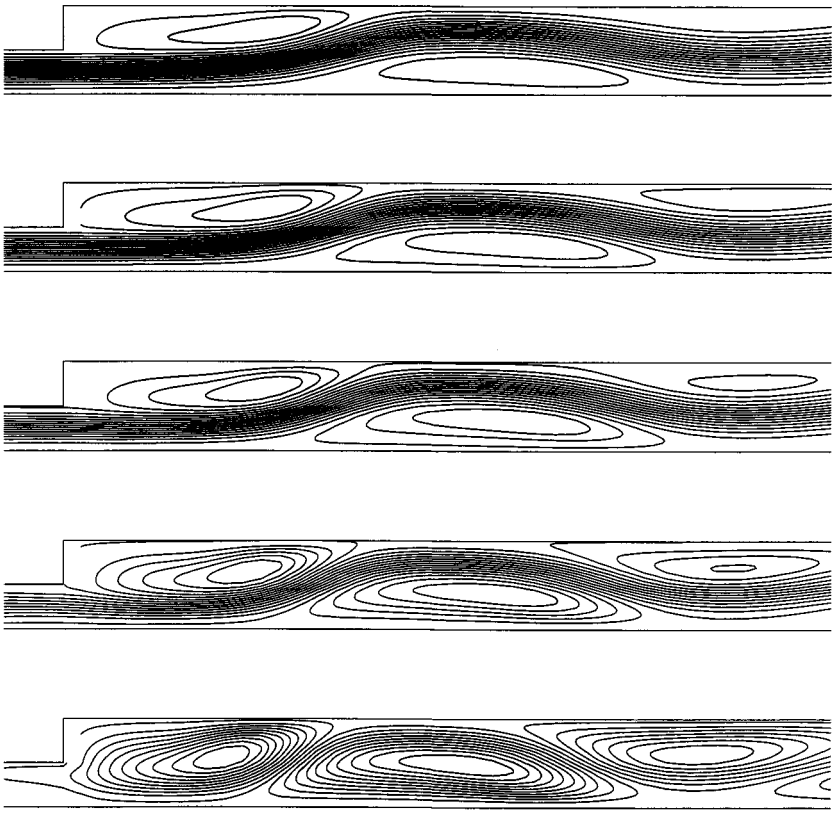

Figure 4. Predictions of the streamlines for the fluctuating flow over a backward-facing step problem. The results are respectively taken from the times at 0.39, 0.42, 0.44. 0.47 and 0.5 s. These results are drawn to a similar scale as the experimental photographic results.

water is modeled where the dynamic viscosity is set to $v = 1 \times 10^{-6}$ m^2 s^{-1} (it is assumed that the water is at a constant 20°C). Figure 4 shows the streamlines for $t = 0.39$, 0.42, 0.44, 0.47 and 0.5 s and therefore, the figure can been compared with the observations made by Sobey. These results are shown in Figure 5 in the form of an artistic impression of the photographic plates. Examining the physics of the flow is an area of future research. The reader is referred to Sobey [59] for a discussion of the possible formation of the vortex wave. The current set of results indicate that there is not a good agreement between the predictions and the experimental results; though there is a similarity in the behaviour of the flow fields. Recirculation regions grow with time, moving very slightly upstream. The vortex structure of the numerical predictions is almost exactly twice the length of the experimental results. In other respects, the numerical predictions are in agreement with the experimental results. For example, the predicted rate of growth of the first three vortices shown in Figure 4 is similar to the experimental results.

The discrepancy in the results has not been identified, the following aspects have examined

1. Grid-independency using a finer grid as well as a higher-order differencing scheme.
2. Inlet Reynolds number variation, the Reynolds number was doubled and halved, surprisingly similar predictions were made. (The length of the recirculation regions does not appear to be directly proportionate to the Reynolds number).

3. Inlet profile, uniform and parabola profiles were tested, as well as setting a constant downward velocity at the inlet to encourage early reattachment.
4. Time step values have been tested, using real time steps of $\Delta t = 2 \times 10^{-4}$, 1×10^{-4} and 5×10^{-5} s.
5. The SIMPLE* scheme has been validated against the PISO scheme, where identical results were obtained.
6. The outlet boundary condition was tested by replacing the outlet boundary extrapolation with first-order approximation of Sommerfeld's equation as well as first-order extrapolation. (The flow changes slowly in the outlet region, and therefore the outlet condition plays an insignificant role).
7. The geometry was varied using a very long inlet channel ($10h$) and a very long main channel ($60h$).

The author can only conclude that an input variable has been incorrectly stated or assumed, or the experimental flow does not behave as a planar flow.

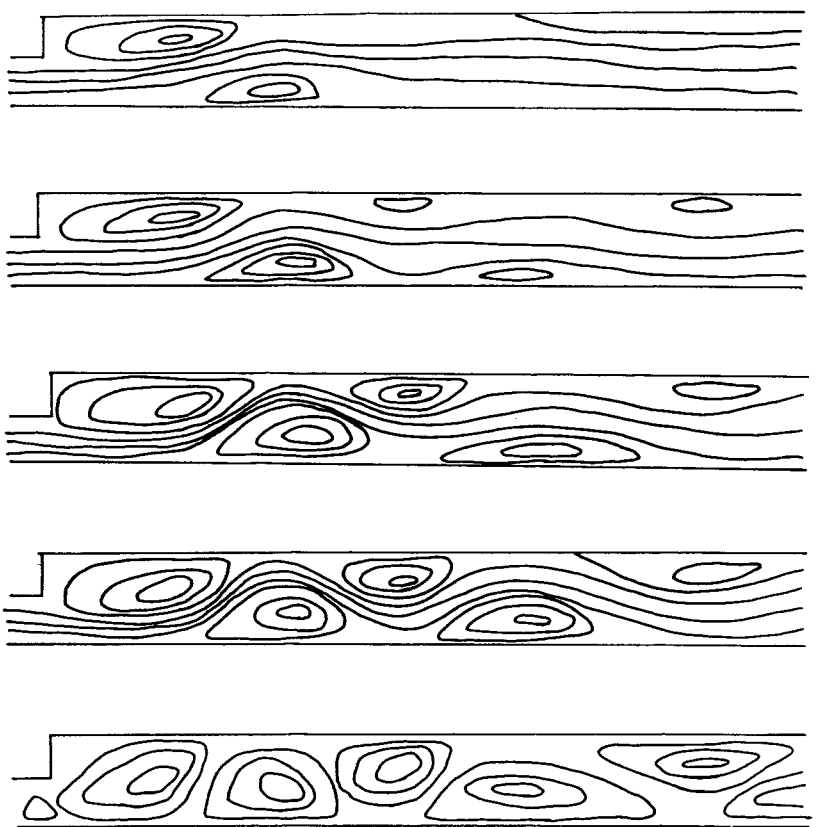

Figure 5. Artistic impression of the streamlines for the fluctuating flow over a backward-facing step problem taken from photographic results. The results are for the same times as Figure 4.

5. CONCLUDING REMARKS

A new scheme, called SIMPLE*, which can solve unsteady incompressible flows has been presented in this paper. The scheme is a SIMPLE variant. Generally speaking, from simulations undertaken, it appears to have a similar accuracy, stability, implicit treatment and computational efficiency as compared with the well-established scheme, PISO. Both schemes predict identical results provided realistic boundary conditions are applied. The advantage of the new scheme is that it does not require velocity correction terms. This is particularly advantageous when dealing with complex differencing schemes, curvilinear or unstructured grid systems.

The novel feature of the new scheme is in using intermediate steps for a single time step. After each intermediate step is calculated, the results are underrelaxed to enhance the stability. An effective way of underrelaxing (damping) the results is described, although, the most efficient method of underrelaxation requires further investigation and will probably be found to be problem-dependent.

The new scheme was used to solve three laminar flow problems. The problems were impulsively started flow over a backward-facing step, flow around a square cylinder and fluctuating flow over a backward-facing step. Comparisons made with numerical and experimental data show good agreement for the first two applications, while only qualitative agreement with the experimental data was achieved for the fluctuating flow over a backward-facing step problem. The cause for the discrepancy was investigated but not identified.

ACKNOWLEDGMENTS

Thanks to Professor J.E. Ffowcs Williams' help and encouragement and to Dr S. Cant for helpful discussions and contributions regarding the numerical methodology. Acknowledgement also to the supervision of Dr A.M. Savill.

REFERENCES

1. F.H. Harlow and J.E. Welch, 'Numerical calculations of time-dependent viscous incompressible flow of fluid with free surface', *Phys. Fluids*, **8**, 2182–2189 (1965).
2. S.V. Patankar and D.B. Spalding, 'A calculation procedure for heat, mass and momentum transfer in three-dimensional parabolic flows', *Int. J. Heat Mass Transf.*, **15**, 1787–1806 (1972).
3. G.D. Raithby and G.E. Schneider, 'Numerical solution of problems in incompressible fluid flow: treatment of the velocity–pressure coupling', *Numer. Heat Transf.*, **2**, 417–440 (1979).
4. J.P. Van Doormaal and G.D. Raithby, 'An evaluation of the segregated approach for predicting incompressible fluid flows', *Natl. Heat Transf. Conf.*, *ASME 85-HT-9*, 1985.
5. R.I. Issa, 'Solution of the implicitly discretized fluid flow equations by operator-splitting', *J. Comput. Phys.*, **62**, 40–65 (1985).
6. L. Guoyan, 'A numerical method of solving two-phase fluid flow', in L. Cheung, S.-K. Lee and K.K. Leung (eds.), *Computational Mechanics*, Balkema, South Korea, 1991, pp. 1589–1594.
7. C.Y. Perng and R.L. Street, 'A coupled multigrid–domain splitting technique for simulating incompressible flows in geometrically complex domains', *Int. J. Numer. Methods Fluids*, **13**, 269–286 (1991).
8. S.L. Lee and R.Y. Tzong, 'Artificial pressure for pressure-linked equation', *Int. J. Heat Mass Transf.*, **35**, 2705–2716 (1992).
9. P. Luchini and A. D'Alascio, 'Multigrid pressure correction techniques for the computation of quasi-incompressible internal flows', *Int. J. Numer. Methods Fluids*, **48**, 489–507 (1994).
10. L. Cheng and S. Armfield, 'A simplified marker and cell method for unsteady flows on non-staggered grids', *Int. J. Numer. Methods Fluids*, **21**, 15–34 (1995).
11. S. Ratan and J. Rodriguez, 'Transient dynamic analysis of rotors using SMAC techniques: Part I Formulation', *Trans. ASME J. Vib. Acoust.*, **114**, 477–488 (1992).
12. P. Orlandi, 'Vorticity–velocity formulation for high *Re* flows', *Comput. Fluids*, **15**, 137–149 (1987).

13. G. Guj and F. Stella, 'Numerical solutions of high-*Re* recirculating flows in vorticity-velocity form', *Int. J. Numer. Methods Fluids*, **8**, 405–416 (1988).
14. L.S. Caretto, A.D. Gosman, S.V. Patankar and D.B. Spalding, 'Two calculation procedures for steady, three-dimensional flows with recirculation', *Proc. 3rd Int. Conf. Numer. Methods in Fluid Dynamics*, Paris, 1972.
15. J.P. Van Doormaal and G.D. Raithby, 'Enhancements of the SIMPLE method for predicting incompressible fluid flows', *Numer. Heat Transf.*, **7**, 147–163 (1984).
16. S.V. Patankar, *Numerical Heat Transfer and Fluid Flow*, Hemisphere, Washington D.C, 1980.
17. A. Wanik and U. Schnell, 'Some remarks on the PISO and SIMPLE algorithms for steady turbulent flow problems', *Comput. Fluids*, **17**, 555–570 (1989).
18. J.J. McGuirk and J.M.L.M. Palma, 'The effciency of alternative pressure–correction formulations for incompressible turbulent flow problems', *Comput. Fluids*, **22**, 77–87 (1993).
19. H. Stroll, F. Durst, M. Peric, J.C.F. Pereira and G. Scheuerer, 'Study of laminar, unsteady piston-cylinder flows', *Trans. ASME. J. Fluids Eng.*, **115**, 687–693 (1993).
20. I.E. Barton, 'Comparison of SIMPLE and PISO type schemes for transient flows', *Int. J. Numer. Methods Fluids*, **26**, 459–483 (1998).
21. I.E. Barton, 'A numerical investigation of incompressible dilute particulate flows', *Ph.D. Thesis*, Aerospace Division, School of Engineering, University of Manchester, Manchester, UK, 1995.
22. R.I. Issa, B. Ahmadi-Befrui, K.R. Beshay and A.D. Gosrnan, 'Solution of the implicitly discretised reacting flow equations by operator-splitting', *J. Comp. Phys.*, **93**, 388–410 (1991).
23. G.D. Thiart, 'Finite difference scheme for the numerical solution of fluid flow and heat transfer problems on non-staggered grids', *Numer. Heat Transf. B*, **17**, 43–62 (1990).
24. C.Y. Perng and R.L. Street, 'Three-dimensional unsteady flow simulations: alternative strategies for a volume averaged calculation', *Int. J. Numer. Methods Fluids*, **9**, 341–362 (1989).
25. W. Shyy and C.S. Sun, 'Development of a pressure-correction/staggered-grid based multigrid solver for incompressible recirculating flows', *Comput. Fluids*, **22**, 51–76 (1993).
26. C.R. Maliska and G.D. Raithby, 'A method for computing three-dimensional flows using non-orthogonal boundary-fitted co-ordinates', *Int. J. Numer. Methods Fluids*, **4**, 519–537 (1984).
27. P. Tamamidis and D.N. Assanis, 'Prediction of three-dimensional steady incompressible flows using body fitted co-ordinates', *Trans. ASME J. Fluids Eng.*, **115**, 457–462 (1993).
28. M.M. Grigor'ev, 'A boundary element formulation using the SIMPLE method', *Int. J. Numer. Methods Fluids*, **16**, 549–579 (1993).
29. B.R. Latimer and A. Pollard, 'Comparison of pressure–velocity coupling solution algorithms', *Numer. Heat Transf.*, **8**, 635–652 (1985).
30. S.V. Patankar, 'Recent developments in computational heat transfer', *Trans. ASME J. Heat Transf.*, **110**, 1037–1045 (1988).
31. J. Simoneau and A. Pollard, 'Finite volume methods for laminar and turbulent flows using a penalty function approach', *Int. J. Numer. Methods Fluids*, **18**, 733–746 (1994).
32. D.M. Wang, A.P. Watkins and R.S. Cant, 'Three-dimensional diesel engine combustion simulation with a modified EPISO procedure', *Numer. Heat Transf. A*, **24**, 249–272 (1993).
33. D.M. Wang and A.P. Watkins, 'Numerical modelling of diesel spray wall impaction phenomena', *Int. J. Heat Fluid Flow*, **14**, 301–312 (1993).
34. W.K. Chow and N.K. Fong, 'Application of field modelling technique to simulate interaction of sprinkler and fire-induced smoke layer', *Combust. Sci. Technol.*, **89**, 101–151 (1993).
35. J.K. Dukowicz, 'A particle-fluid numerical model for liquid sprays', *J. Comput. Phys.*, **35**, 229–253 (1980).
36. M.K. Patel and N.C. Markatos, 'An evaluation of eight discretization schemes for two-dimensional convection–diffusion equations', *Int. J. Numer. Methods Fluids*, **6**, 129–154 (1986).
37. C.A.J. Fletcher, *Computational Techniques for Fluid Dynamic*, vol. II, Springer, Berlin, 1988.
38. D.A. Anderson, J.C. Tannehill and R.H. Pletcher, *Computational Fluid Mechanics and Heat Transfer*, Hemisphere, Washington D.C., 1984.
39. C. Hirsch, *Numerical Computation of Internal and External Flows, Vol. 1: Fundamentals of Numerical Discretization*, Wiley, New York, 1989.
40. W. Shyy, 'A study of finite difference approximations to steady state, convection-dominated flow problems', *J. Comput. Phys.*, **57**, 415–438 (1985).
41. D.B. Spalding, 'A novel finite difference formulation for differential expressions involving both first- and second-derivatives', *Int. J. Numer. Methods Eng.*, **4**, 551–559 (1972).
42. M. Peric, 'A finite volume method for the prediction of three-dimensional fluid flow in complex ducts', *Ph.D. Thesis*, Mechanical Engineering Department, Imperial College, London, UK, 1985.
43. S.W. Kim and T.J. Benson, 'Comparison of the SMAC, PISO and iterative time-advancing schemes for unsteady flows', *Comput. Fluids*, **21**, 435–454 (1992).
44. B.F. Armaly, F. Durst, J.C.F. Pereira and B. Schonung, 'Experimental and theoretical investigation of backward-facing step flow', *J. Fluid Mech.*, **127**, 473–496 (1983).
45. S. Thangam and D.D. Knight, 'Effect of step height on the separated flow past a backward-facing step', *Phys. Fluids A*, **1**, 604–606 (1989).

46. J. Kim and P. Moin, 'Application of a fractional step method to incompressible Navier–Stokes equations', *J. Comput. Phys.*, **59**,308–323 (1985).
47. J.L. Sohn, 'Evaluation of FIDAP on some classical laminar and turbulent benchmarks', *Int. J. Numer. Methods Fluids*, **8**, 1469–1490 (1988).
48. D.K. Gartling, 'A test problem for outflow boundary conditions flow over a backward-facing step', *Int. J. Numer. Methods Fluids*, **11**, 953–967 (1990).
49. D. Lee and Y.M. Tsuei, 'A modified adaptive grid method for recirculating flows', *Int. J. Numer. Methods Fluids*, **14**, 775–791 (1992).
50. R.L. Sani and P.M. Gresho, 'Resume and remarks on the open boundary condition minisymposium', *Int. J. Numer. Methods Fluids*, **18**, 983–1008 (1994).
51. I.E. Barton, 'A numerical study of flow over a confined backward facing step', *Int. J. Numer. Methods Fluids*, **21**, 653–665 (1995).
52. P.M. Gresho, 'Letter to the editor', *Numer. Heat Transf. A*, **20**, 123 (1991).
53. P.M. Gresho, D.K. Gartling, J.R. Torczynski, K.A. Cliffe, K.H. Winters, T.J. Garrat, A. Spence and J.W. Goodrich, 'Is the steady viscous incompressible two-dimensional flow over a backward-facing step at $Re = 800$ stable?', *Int. J. Numer. Methods Fluids*, **17**, 501–541 (1993).
54. I.E. Barton, 'The computation of the entrance effect for laminar flow over a backward-facing step', *Int. J. Numer. Methods Fluids*, **25**, 633–644 (1997).
55. F. Durst and J.C.F. Pereira, 'Time-dependent laminar backward-facing step flow in a two-dimensional duct', *Trans. ASME J. Fluids Eng.*, **110**, 289–296 (1988).
56. R.W. Davis and E.F. Moore, 'A numerical study of vortex shedding from rectangles', *J. Fluid Mech.*, **116**, 475–506 (1982).
57. P.M. Gresho and S.T. Chan, 'On the theory of semi-implicit projection methods for viscous incompressible flow and its implementation via a finite element method that also introduces a nearly consistent mass matrix. Part 2: Implementation', *Int. J. Numer. Methods Fluids*, **11**, 621–659 (1990).
58. B. Ramaswamy, 'Theory and implementation of a semi-implicit finite element method for viscous incompressible flow', *Comput. Fluids*, **22**, 725–747 (1993).
59. I.J. Sobey, 'Observation of waves during oscillatory channel flow', *J. Fluid Mech*, **151**, 395–426 (1985).

